

1 **Why FIT and bHLH Ib interdependently regulate Fe-uptake**

2

3 Yuerong Cai^{a, b, c}, Yujie Yang^{a, b, c}, Huaqian Ping^{a, b}, Chengkai Lu^a, Rihua Lei^{a, b},
4 Yang Li^a, Gang Liang^{a, b*}

5

6 ^aCAS Key Laboratory of Tropical Plant Resources and Sustainable Use,
7 Xishuangbanna Tropical Botanical Garden, Chinese Academy of Sciences,
8 Kunming, Yunnan 650223, China

9 ^bThe College of Life Sciences, University of Chinese Academy of Sciences,
10 Beijing 100049, China

11 ^c The authors contributed equally to this work

12 *Correspondence:

13 Gang Liang

14 Email: lianggang@xtbg.ac.cn

15

16 **Running title:**

17 FIT and bHLH Ib in Fe uptake

18

19

20 **Abstract**

21 FIT (FER-LIKE IRON DEFICIENCY- INDUCED TRANSCRIPTION FACTOR)
22 and four bHLH 1b transcription factors (TFs) bHLH38, bHLH39, bHLH100 and
23 bHLH101, are the master regulators of Fe uptake genes, and they interact
24 with each other to activate the Fe uptake systems. However, it remains
25 unclear why FIT and bHLH 1b depend on each other to regulate the Fe
26 deficiency response. By analyzing Fe deficiency phenotypes and Fe uptake
27 genes, we found that the quadruple *bhlh4x* mutants (*bhlh38 bhlh39 bhlh100*
28 *bhlh101*) mimic the *fit* mutant. Subcellular localization analyses indicate that
29 bHLH38 and bHLH39 are preferentially expressed in the cytoplasm whereas
30 bHLH100 and bHLH101 in the nucleus. Transcriptome data show that the
31 genes involved in Fe signaling pathway show the same expression trends in
32 *bhlh4x* and *fit*. Genetic analyses suggest that FIT and bHLH 1b depend each
33 other to regulate the Fe deficiency response. Further biochemical assays
34 indicate that bHLH 1b TFs possess the DNA binding ability and FIT has the
35 transcription activation ability. This work concludes that FIT and bHLH 1b form
36 a functional transcription complex in which bHLH 1b is responsible for target
37 recognition and FIT for transcription activation, explaining why FIT and bHLH
38 1b interdependently regulate Fe uptake.

39 Introduction

40 Fe is one of the micronutrients crucial for plant growth and development
41 because Fe acts as a cofactor involved in chlorophyll biosynthesis,
42 photosynthesis, respiration, and other biochemical reactions. Fe deficiency
43 often leads to Fe-deficiency symptoms such as interveinal chlorosis in leaves
44 and reduction of crop yields. Plants absorb Fe from soil; however, Fe
45 acquisition is challenging due to the low solubility of Fe in soil solution
46 (Guerinot and Yi, 1994).

47 The requirement for efficient acquisition of Fe from soil has led to the
48 evolution of two distinct uptake strategies, strategy I in non-graminaceous
49 plants and strategy II in graminaceous plants (Marschner & Romheld, 1986;
50 Romheld & Marschner, 1986; Grillet & Schmidt, 2019). Arabidopsis plants
51 employ the strategy I which involves three sequential steps, mobilization of
52 ferric Fe, reduction of ferric Fe, and transport of ferrous Fe. Insoluble ferric Fe
53 is mobilized by acidification of the rhizosphere resulting from protons secreted
54 by AHA2, a proton ATPase (Santi and Schmidt, 2009) and by phenolic
55 compounds (Rodríguez-Celm et al., 2013; Schmid et al., 2014; Fourcroy et al.,
56 2016; Tsai et al., 2018). Ferric Fe is then reduced to ferrous Fe by FRO2
57 (FERRIC REDUCTION OXIDASE 2) (Robinson et al., 1999), and finally
58 translocated into roots by epidermis localized IRT1 (IRON-REGULATED
59 TRANSPORTER 1) (Varotto et al., 2002; Vert et al., 2002).

60 FIT is a key regulator of strategy I since its loss-of-function causes
61 reduction of Fe uptake genes including *IRT1* and *FRO2* and severe Fe
62 deficiency symptoms (Colangelo & Guerinot, 2004; Jakoby et al., 2004; Yuan
63 et al., 2005; Schwarz & Bauer, 2020). Interestingly, early reports showed that
64 the singular overexpression of *FIT* does not result in constitutive activation of
65 *IRT1* and *FRO2* (Colangelo & Guerinot, 2004; Jakoby et al., 2004). Later
66 studies revealed that FIT interacts with each of four bHLH Ib transcription
67 factors (TFs), bHLH38/39/100/101, and dual overexpression of bHLH Ib and
68 *FIT* constitutively activates *IRT1* and *FRO2* (Yuan et al., 2008; Wang et al.,

69 2013), implying that FIT and bHLH Ib TFs function synergistically. Unlike
70 singular *FIT* overexpression, singular overexpression of *bHLH39* (or
71 *bHLH101*) activates the expression of *IRT1* and *FRO2* (Yuan et al., 2008;
72 Wang et al., 2013). However, Naranjo-Arcos et al. (2017) revealed that the
73 activation of *IRT1* and *FRO2* by *bHLH39* overexpression disappears in the
74 absence of FIT, implying that bHLH Ib functions in a FIT dependent fashion.
75 All four bHLH Ib members are significantly upregulated in the *fit* mutant
76 (Wang et al., 2007), further supporting that FIT is required for bHLH Ib
77 activating *IRT1* and *FRO2*. It is unclear whether FIT can function
78 independently of bHLH Ib. Therefore, it is particularly of importance to clarify
79 the molecular mechanism by which FIT and bHLH Ib TFs coordinate the
80 expression of Fe uptake genes with the fluctuation of Fe availability.

81 Wang et al. (2013) revealed that the induction of *IRT1* and *FRO2* by Fe
82 deficiency is decreased in the *bhlh138 bhlh100 bhlh101* and *bhlh139 bhlh100*
83 *bhlh101* mutants. In contrast, Sivitz et al. (2012) and Maurer et al. (2014)
84 revealed that the expression of *IRT1* and *FRO2* is not affected in the *bhlh100*
85 *bhlh101* and *bhlh139 bhlh100 bhlh101* mutants. Unlike *FIT* that is a
86 root-specific gene, all four bHLH Ib genes are ubiquitously expressed both in
87 the root and shoot under Fe deficiency conditions (Wang et al., 2007). A
88 previous study concluded that bHLH Ib genes are involved in the leaf cell
89 differentiation and chloroplast development (Andriankaja et al., 2014). It
90 remains unclear whether bHLH Ib TFs have specific roles in regulating Fe
91 deficiency response of shoots. Due to the functional redundancy of bHLH Ib
92 members, functional clarification of bHLH Ib genes calls for the generation of
93 their quadruple mutants. It is also an open question whether FIT and bHLH Ib
94 have the identical contribution to the expression of Fe uptake genes.

95 In this study, we aimed to clarify whether FIT and bHLH Ib have the same
96 functions in regulating Fe uptake and how they coordinate the expression of
97 Fe uptake genes in the shoots and roots. We found that *fit* and *bhlh4x* (*bhlh38*
98 *bhlh39 bhlh100 bhlh101*) mutants have the identical Fe deficiency symptoms.

99 Further transcriptome analysis revealed that they affect the expression of Fe
100 uptake genes in the same way. Genetic evidence suggested that FIT and
101 bHLH 1b function in the same genetic node. Further biochemical analysis
102 found that bHLH 1b TFs without transcription activation activity have DNA
103 binding activity and FIT without DNA binding activity has transcription
104 activation activity. This work reveals that FIT and bHLH 1b form a functional
105 transcription complex to activate the expression of Fe uptake genes.

106 **Results**

107 **bHLH Ib quadruple mutants phenocopy the *fit* loss-of-function mutant**

108 To avoid the functional redundancy between the four bHLH Ib members, we
109 constructed the *bhlh38 bhlh39 bhlh100 bhlh101* (*bhlh4x*) quadruple mutants
110 by editing *bHLH39* with CRISPR/Cas9 in the *bhlh38 bhlh100 bhlh101*
111 background. When grown in soil, both *bhlh4x* and *fit-2* died at the seedling
112 stage and this phenomenon could be rescued by extra Fe application (Figure
113 1A). The Fe concentration in *bhlh4x* was similar to that in *fit-2*, but
114 significantly lower than that in wild type (Figure 1B). When grown on Fe
115 deficient agar medium, *bhlh4x* and *fit-2* produced similar chlorotic leaves and
116 short roots (Supplemental Figure S1A). In agreement with the chlorotic leaves,
117 the chlorophyll concentration in both *bhlh4x* and *fit-2* was remarkably reduced
118 (Supplemental Figure S1B). Next, we analyzed the H⁺-ATPase activity and
119 ferric-chelate reductase activity, the typical indicators of Fe deficiency (Yi and
120 Guerinot, 1996; Fox and Guerinot, 1998). In contrast to the visible coloration
121 around the wild type roots, the coloration was hardly observed around the
122 *bhlh4x* and *fit-2* roots (Figure 1C). Similarly, the ferric-chelate reductase
123 activity was not increased significantly in both *bhlh4x* and *fit-2* under Fe
124 deficient conditions (Figure 1D). Subsequently, we determined the expression
125 of *IRT1* and *FRO2*, finding that their expression levels were similar between
126 *bhlh4x* and *fit-2* (Figure 1E and F). Collectively, no matter under Fe sufficient
127 or deficient conditions, the *bhlh4x* mutants completely mimicked *fit-2*.

128

129 **FIT and bHLH Ib act in the same genetic node of Fe signaling pathway**

130 To analyze how FIT and bHLH Ib TFs regulate the Fe deficiency response,
131 we investigated transcriptomic changes in the *fit-2* and *bhlh4x*. Seven-day-old
132 seedlings grown on Fe sufficient medium were shifted to Fe sufficient or
133 deficient medium for 3 days, respectively. Shoots and roots were harvested
134 separately for RNA sequencing. We identified 864 genes upregulated by Fe
135 deficiency in a FIT dependent manner in roots, 66% of which also depended

136 on bHLH Ib TFs (Figure 2A). Similarly, we identified 550 genes
137 downregulated by Fe deficiency in a FIT dependent manner in roots, 60% of
138 which also depended on bHLH Ib TFs (Figure 2A). Then, we focused on the
139 expression of the well-known Fe deficiency responsive genes in roots. We
140 found that the FIT dependent Fe-uptake associated genes, such as *IRT1*,
141 *IRT2*, *FRO2*, *NICOTIANAMINE SYNTHASE 1 (NAS1)*, *NAS2*, *IRON*
142 *REGULATED 2 (IREG2)*, *ZRT- AND IRT-RELATED PROTEIN 8 (ZIP8)*, *ZIP9*,
143 *MYB10*, *MYB72*, *SCOPOLETIN 8-HYDROXYLASE (S8H)*, *CYTOCHROME*
144 *P450, FAMILY 82, SUBFAMILY C, POLYPEPTIDE 4 (CYP82C4)*, etc, were
145 down-regulated in *fit-2* and *bhlh4x*, whereas the FIT independent Fe
146 deficiency responsive genes, such as *IRON MAN 1-4 (IMA1-4)*, *IMA6*, *FRO3*,
147 *OLIGOPEPTIDE TRANSPORTER 3 (OPT3)*, *BRUTUS (BTS)*, *POPEYE*
148 *(PYE)*, etc, were up-regulated in *fit-2* and *bhlh4x* (Figure 2B; Supplemental
149 Table S1). These data suggest that bHLH Ib TFs regulate the Fe deficiency
150 response of roots in a manner similar to FIT. Under Fe deficient conditions,
151 *FIT* is mainly expressed in the root (Jakoby et al., 2004), and bHLH Ib TFs are
152 abundant in both the root and shoot (Wang et al., 2007). However, the shoots
153 of *bhlh4x* and *fit-2* displayed the identical phenotypes (Figure 1A;
154 Supplemental Figure S1), and the typical Fe-deficiency responsive genes
155 showed the very similar change trends in the shoots of *bhlh4x* and *fit-2* in
156 response to Fe deficiency (Supplemental Figure S2; Supplemental Table S2).
157 Given that FIT and bHLH Ib TFs affect the expression of Fe deficiency
158 responsive genes in a similar fashion, we proposed that they act in the same
159 genetic node of Fe deficiency response signaling pathway. To further confirm
160 this hypothesis, we generated *bhlh4x-2 fit-2* quintuple mutants by crossing
161 *bhlh4x-2* with *fit-2*. No matter in normal soil or in soil supplied with extra Fe,
162 there is no visible difference between *bhlh4x-2*, *fit-2*, and *bhlh4x-2 fit-2*
163 (Supplemental Figure S3). These results suggest that bHLH Ib and FIT play
164 the same roles in Fe homeostasis.

166 **Overexpression of *FIT* cannot rescue *bhlh4x***

167 The four bHLH Ib members are significantly up-regulated in the *fit* mutant
168 (Wang et al., 2007), implying that FIT is not required for the upregulation of
169 bHLH Ib genes. The activation of *IRT1* and *FRO2* by *bHLH39* overexpression
170 disappears in the absence of FIT (Naranjo-Arcos et al., 2017), implying that
171 the functions of bHLH Ib TFs require the involvement of FIT. To further
172 confirm whether the function of FIT requires bHLH Ib TFs, we generated the
173 *FIT* overexpression plants (*bhlh4x/FIToe*) in the *bhlh4x-1* background.
174 Irrespective of Fe status, the overexpression of *FIT* had no effect on the
175 phenotypes of *bhlh4x-1*, as well as on the expression of *IRT1* and *FRO2* in
176 the *bhlh4x-1* (Figure 3). Together, all these data suggest the functional
177 interdependence between FIT and bHLH Ib in the Fe deficiency response.

178

179 **Subcellular localization of bHLH Ib members**

180 The phenotypic and genetic data support that FIT and bHLH Ib TFs depend
181 on each other to function. Next, we explored why FIT and bHLH Ib require
182 each other to function. A recent study revealed that bHLH39 moves to nuclei
183 in a FIT dependent manner (Trofimov et al., 2019). Thus, it is likely that the
184 bHLH Ib TFs need FIT to help them accumulate in nuclei and then activate
185 Fe-uptake genes. To test this hypothesis, we fused the mCherry reporter to
186 the C-end of bHLH Ib members and conducted transient expression assays
187 (Figure 4A). Like bHLH39-mCherry, bHLH38-mCherry was mainly expressed
188 in the cytoplasm. To determine the localization of bHLH38-mCherry in the
189 presence of FIT, the GFP reporter was fused to the C-end of FIT. Unlike the
190 GFP alone which was highly expressed in both the cytoplasm and nucleus,
191 FIT-GFP was mainly expressed in the nucleus. The localization of
192 bHLH38-mCherry did not change when co-expressed with the GFP. In
193 contrast, most of bHLH38-mCherry was observed in the nucleus when
194 co-expressed with the FIT-GFP (Figure 4B). This scenario is very similar to
195 the case of bHLH39 (Trofimov et al., 2019). However, bHLH100-mCherry and

196 bHLH101-mCherry were observed mainly in the nucleus in the absence of
197 FIT (Figure 4A). Given the functional redundancy of bHLH Ib TFs and nuclear
198 localization of bHLH100 and bHLH101 without the FIT assistance, we
199 speculated that the FIT dependent nuclear accumulation of bHLH38 and
200 bHLH39 is not the reason why bHLH Ib functionally depends on FIT.

201

202 **bHLH Ib TFs have DNA binding ability, but no transactivation ability**

203 Generally, eukaryotic TFs contain at least two domains, a DNA binding
204 domain and a transcriptional activation or repression domain, which operate
205 together to control the transcriptional initiation from target gene promoters.
206 Subsequently, we wanted to know if FIT and bHLH Ib have the two
207 characteristic domains. We employed an artificial GAL4 reporter system
208 (Figure 5A), in which the yeast *GAL4* promoter (*pGAL4*) was used to drive a
209 nuclear localization signal fused GFP (nGFP) as the reporter (*pGAL4:nGFP*)
210 and the GAL4 DNA binding domain (BD) with a nuclear localization signal
211 fused mCherry (nmCherry) was linked with a test protein X as the effector
212 (BD-nmCherry-X). A strong transactivation domain VP16 from the herpes
213 simplex virus was used as a positive control. Similar to the positive control,
214 FIT activated the expression of *nGFP* whereas all four bHLH Ib TFs did not
215 (Figure 5B). These data suggest that FIT, but not the four bHLH Ib TFs, has
216 the transcriptional activation ability.

217

218 **FIT has transactivation ability, but no DNA binding ability**

219 Subsequently, we wanted to know whether they have the DNA binding ability.
220 It is well known that the bHLH domain of bHLH TFs is responsible for DNA
221 binding and the amino acids at positions 5, 9, and 13 in the basic region are
222 the most critical (Heim et al., 2003). The bHLH proteins with DNA binding
223 ability have the conserved H/K-E-R residues at positions 5, 9, and 13 (Heim
224 et al., 2003; Liu et al., 2013; Zhang et al., 2017, 2020; Lei et al., 2020). We
225 aligned the bHLH domain of FIT and bHLH Ib, and found that the four bHLH

226 Ib TFs share an H-E-R motif, but FIT has a T-E-R motif (Figure 6A), implying
227 that FIT may have no DNA binding ability. To provide experimental evidence,
228 electrophoretic mobility shift assays (EMSA) were conducted. His-tagged
229 bHLH38/39 and FIT were respectively expressed and purified from
230 *Escherichia coli* and a fragment of *IRT1* promoter with an E-box was used the
231 probe. The results suggest that bHLH38/39 can bind to the promoter of *IRT1*
232 whereas FIT cannot (Figure 6B). Taken together, our data suggest that FIT
233 has transcriptional activation ability and bHLH Ib has DNA binding ability. We
234 propose that bHLH Ib and FIT form a functional transcription complex, in
235 which bHLH Ib is responsible for target DNA binding and FIT for transcription
236 activation.

237

238 **FIT and bHLH Ib form a functional transcription complex**

239 We proposed that bHLH Ib and FIT form a functional transcription complex, in
240 which bHLH Ib is responsible for target DNA binding and FIT for transcription
241 activation. It has been confirmed that the activation of *IRT1* and *FRO2* by
242 bHLH39 requires the involvement of FIT (Naranjo-Arcos et al., 2017). Given
243 that FIT interacts with bHLH Ib and the latter directly binds to the promoter of
244 *IRT1*, we wondered whether the FIT-bHLH Ib complex associates with the
245 promoter of *IRT1* *in vivo*. CHIP assays were performed in parallel among wild
246 type, *FIToe* and *bhh4x-1/FIToe*. We observed FIT-specific enrichment for the
247 *IRT1* promoter in the *FIToe* plants. However, this enrichment was dramatically
248 reduced in the *bhh4x-1/FIToe* plants (Figure 7A). These data suggest that
249 bHLH Ib is required for FIT association with target promoters.

250 Although bHLH Ib genes are highly expressed in the shoots under Fe
251 deficient conditions, the Fe-uptake genes (e. g. *IRT1*) are barely expressed.
252 Having confirmed that FIT and bHLH Ib depend each other to initiate the
253 transcription of their target genes, we wondered whether the expression of
254 Fe-uptake genes would increase dramatically under Fe deficiency conditions
255 if *FIT* was ectopically overexpressed in the shoots. To test this hypothesis, we

256 determined the expression of *IRT1* and *FRO2* in the *FIToe* plants (Figure 7B).
257 In consistence with the high levels of *FIT* mRNA, the abundance of *IRT1* and
258 *FRO2* was also at a considerably high level in the shoot of *FIToe* under Fe
259 deficient conditions. Collectively, these results support that FIT and bHLH Ib
260 form a functional transcription complex to activate the expression of Fe
261 uptake genes.

262 **Discussion**

263 The transcription activation of Fe uptake genes and then Fe uptake is crucial
264 for plants' survival upon Fe deficiency conditions. FIT is a regulatory hub for
265 iron deficiency and stress signaling in roots, which determines the expression
266 of Fe uptake genes with the fluctuation of Fe status (Schwarz & Bauer, 2020).
267 Two important questions regarding FIT and bHLH Ib are why they depend on
268 each other to regulate Fe uptake, and whether they have their own
269 independent functions in Fe signaling. Here, we address these two questions
270 by physiological, genetic, and molecular evidence.

271 Although bHLH Ib genes are required for the expression of Fe uptake
272 genes, their functional redundancy and lack of mutants with the
273 loss-of-function of all four members make it hard to elucidate their exact
274 contribution to Fe uptake. In terms of the Fe deficiency response, *fit-2* and
275 *bhlh4x* mutants displayed the identical phenotypes as well as the same
276 expression trends of Fe signaling associated genes, suggestive of the equal
277 contribution of FIT and bHLH Ib to the Fe deficiency response. It was reported
278 that the bHLH Ib member bHLH39 has no influence on the Fe-uptake genes
279 in the absence of FIT (Naranjo-Arcos et al., 2017). We further confirmed that
280 FIT cannot affect the Fe-uptake genes without bHLH Ib (Figure 3). These
281 data suggest that FIT and bHLH Ib interdependently regulate the Fe-uptake
282 genes.

283 Generally, a TF consists of a DNA binding domain and a transcription
284 activation/repression domain. However, some TFs lost one of these two
285 domains. For instance, IBH1 (ILI1 binding bHLH1) TF has no DNA binding
286 ability, but interacts with ACEs (bHLH transcriptional activators for cell
287 elongation) and interferes with the DNA binding ability and the transcription
288 activation activity of the latter (Ikeda et al., 2012). In Arabidopsis, several
289 single-repeat R3-MYB TFs, such as TRY (Triptychon), CPC (Caprice), ETCs
290 (Enhancer of TRY and CPC 1, 2, 3), act as negative regulators of trichome
291 differentiation, which contain a single DNA binding domain, but lack the

292 activation domain (Wang and Chen, 2014). Here, we show that FIT has no
293 DNA binding domain and bHLH 1b no transcription activation domain, and
294 they both complement each other to form a functional transcription complex
295 to initiate the transcription of their target genes. This two-component model
296 (Figure 8) rationally explains why the overexpression of one of both cannot
297 activate their targets in the absence of the other (Figure S4; Naranjo-Arcos et
298 al., 2017) and why *bhlh4x* phenocopies *fit* (Figure 1; Figure S1).

299 It is well known that the expression of Fe-uptake genes changes
300 spatio-temporally in response to Fe status. As the positive regulators of
301 Fe-uptake genes, bHLH 1b TFs are ubiquitously expressed in the roots and
302 shoots in response to Fe deficiency. In contrast, the Fe-uptake genes (e. g.
303 *IRT1* and *FRO2*) are highly expressed in the Fe deficient roots, but hardly
304 expressed in the Fe deficient shoots. The working model of FIT and bHLH 1b
305 gives a reasonable explanation to the differential expression patterns of Fe
306 uptake genes and bHLH 1b. In the Fe deficient shoots, although the transcript
307 abundance of bHLH 1b is at a high level, that of *FIT* is at a low level, hence
308 resulting in less FIT-bHLH 1b dimmers and then less Fe-uptake genes. Under
309 Fe sufficient conditions, the Fe-uptake genes are not activated in the roots
310 because bHLH 1b genes are expressed at a low level. Therefore, FIT is the
311 limitation factor for Fe-uptake genes in the shoot, and bHLH 1b is the limitation
312 factor in the roots.

313 The previous studies have revealed that bHLH 1b TFs regulate cell
314 differentiation and chloroplast development (Andriankaja et al., 2014), in
315 agreement with their expression in leaves. In contrast, *FIT* is barely
316 expressed in leaves irrespective of Fe status. We noted that both *fit-2* and
317 *bhlh4x* mutants produced leaves with serrate margin (Figure 1A), implying
318 that FIT might also function in leaf development. Four bHLH 1b genes are
319 involved in Fe uptake in Arabidopsis whereas only one (*OsiRO2*,
320 IRON-RELATED BHLH TRANSCRIPTION FACTOR 2) in rice. bHLH38/39
321 are mainly localized in the cytoplasm and bHLH100/101 in the nucleus.

322 Similar to bHLH100/101, OsIRO2 is also preferentially localized in the
323 cytoplasm. Interestingly, the cytoplasm localized bHLH Ib proteins
324 accumulate in the nucleus in the presence of their interaction partner FIT
325 (Figure 3; Trofimov et al., 2019; Liang et al., 2020; Wang et al., 2020). Further
326 investigation is needed to clarify whether the property of cytoplasmic
327 localization is required for the molecular functions of bHLH Ib proteins.

328 In summary, the genetic and molecular data presented in this study
329 suggest that the physical interaction of FIT and bHLH Ib leads to the
330 formation of a functional transcription activation complex in which bHLH Ib
331 exerts the DNA binding function and FIT exerts the transactivation function
332 (Figure 8). This model explains why FIT and bHLH Ib depend on each other
333 to activate the expression of Fe uptake genes, providing insights into the
334 molecular mechanism by which plants control the expression of Fe-uptake
335 genes in response to Fe deficiency.

336 **Materials and Methods**

337 **Plant materials and growth conditions**

338 *Arabidopsis thaliana* ecotype Col-0 was used as the wide-type. Seeds were
339 surface-sterilized with 20% commercial bleach for 15 min and then washed
340 three times with distilled water. After plated on half MS media, seeds were
341 vernalized for 2 d at 4°C before germination in greenhouse. The ordinary
342 medium was the half MS with 1% sucrose, 0.7% agar A, 0.1 mM Fe-EDTA at
343 pH 5.8. For Fe deficiency media, the same half MS without Fe-EDTA was
344 used. Plates were placed in a culture room at 22°C under a 16 h light/8 h dark
345 photoperiod. *fit-2* (SALK_126020), *bhlh4x-1* and *bhlh4x-2* were described
346 previously (Cai et al., 2021). The identification of *bhlh4x-1 fit-2* is shown in
347 Supplemental Figure S3.

348

349 **High-throughput sequencing of mRNA, and differential gene expression** 350 **analysis**

351 For global analysis of gene expression, roots of wild-type, *bhlh4x-1* and *fit-2*
352 plants grown on +Fe for 4 days and transferred to –Fe for 3 days. Roots and
353 shoot were separately harvested and collected in liquid nitrogen. Total RNA of
354 each sample was extracted according to the instruction manual of the TRIzol
355 Reagent (Life technologies, California, USA). RNA integrity and concentration
356 were checked using an Agilent 2100 Bioanalyzer (Agilent Technologies, Inc.,
357 Santa Clara, CA, USA). The mRNA was isolated by NEBNext Poly (A) mRNA
358 Magnetic Isolation Module (NEB, E7490). The cDNA library was constructed
359 following the manufacturer's instructions of NEBNext Ultra RNA Library Prep
360 Kit for Illumina (NEB, E7530) and NEBNext Multiplex Oligos for Illumina (NEB,
361 E7500). In briefly, the enriched mRNA was fragmented into approximately
362 200nt RNA inserts, which were used to synthesize the first-strand cDNA and
363 the second cDNA. The double-stranded cDNA was performed
364 end-repair/dA-tail and adaptor ligation. The suitable fragments were isolated
365 by Agencourt AMPure XP beads (Beckman Coulter, Inc.), and enriched by

366 PCR amplification. Finally, the constructed cDNA libraries were sequenced on
367 an Illumina sequencing platform. The raw sequencing data are stored in NCBI
368 under the accession number of PRJNA694484
369 (<https://www.ncbi.nlm.nih.gov/sra/PRJNA694484>).

370 The values of fragments per kilobase of transcript per million mapped reads
371 (FPKM) are shown for each gene. The genes for which no hits were recorded
372 across all the samples were discarded from the data set. For the genes
373 whose hits were recorded in only a subset of the samples, we replaced
374 missing values with a small value of expression (0.01 FPKM). Transcript
375 abundance was concluded to increase/decrease under Cu deficiency for a
376 gene when arithmetic means of transcript abundance differed by a factor of at
377 least 2. Changes in transcript levels were concluded to be dependent on FIT
378 if \log_2 FC (wild type -Fe versus fit -Fe) > 1 for \log_2 FC (wild type -Fe versus
379 wild type +Fe) > 1, and \log_2 FC (wild type -Fe versus fit -Fe) < 1 for \log_2 FC
380 (wild type -Fe versus wild type +Fe) < -1. The bHLH lb dependent transcripts
381 were obtained by a similar filtration.

382

383 **Transient expression assays**

384 All related plasmids were transformed into *Agrobacterium tumefaciens* strain
385 EHA105. Agrobacterial cells were infiltrated into leaves of *Nicotiana*
386 *benthamiana* by the infiltration buffer (0.2 mM acetosyringone, 10 mM MgCl₂,
387 and 10 mM MES, pH 5.6). In the transient expression assays, the final optical
388 density at 600 nm value was 0.5 (reporter, pGAL4-nls-GFP) and 0.5 (effector,
389 BD-nmCherry-X). After infiltration 2 days in dark, GFP fluorescence were
390 observed through a Carl Zeiss Microscopy GmbH.

391

392 **EMSA**

393 bHLH38, bHLH39 and FIT were respectively cloned into the pET-28a(+)
394 vector and the resulting plasmids were introduced into *Escherichia coli*
395 BL21(DE3) for protein expression. Cultures were incubated with 0.5 M

396 isopropyl β -D-1-thiogalactopyranoside at 22°C for 16h, and proteins were
397 extracted and purified by using the His-tag Protein Purification Kit (Beyotime,
398 China) following the manufacturer's protocol. EMSA was performed using the
399 Chemiluminescent EMSA Kit (Beyotime, China). For generation of
400 competitive probe (pIRT1) or mutated probe (pIRT1-m), a pair of
401 complementary single-strand DNA primers were synthesized. For generation
402 of the biotin-labeled probe (Biotin-pIRT1), a pair of complementary
403 single-strand DNA primers with a biotin label at the 5' end were synthesized.
404 A pair of complementary primers were used for annealing to form
405 double-strand DNA. The annealing reaction solution for 1 X probe was as
406 follow: 1 μ l of 10 μ M forward prime, 1 μ l of 10 μ M reverse primer, 3 μ l of 10 X
407 Taq buffer, and 25 μ l of H₂O. The annealing reaction solution for 100 X probe
408 was as follow: 10 μ l of 100 μ M forward prime, 10 μ l of 100 μ M reverse primer,
409 3 μ l of 10 X Taq buffer, and 7 μ l of H₂O. Reaction solution was incubated at
410 95°C for 2 minutes, and cool at room temperature. The binding reaction
411 solution was as follow: 5 μ l of H₂O, 2 μ l of 5 X EMSA/Gel-Shift binding buffer,
412 2 μ l of protein, 1 μ l of probe. The competitive binding reaction solution was as
413 follow: 4 μ l of H₂O, 2 μ l of 5 X EMSA/Gel-Shift binding buffer, 2 μ l of protein, 1
414 μ l of 1 X probe, and 1 μ l of 100 X probe. Incubate binding reactions at room
415 temperature for 20 minutes. Add 1 μ l of 10 X Loading Buffer to each 10 μ l
416 binding reaction, pipetting up and down several times to mix. Electrophorese
417 binding reactions in a 6% polyacrylamide gel. Electrophoretic transfer in 0.5 X
418 TBE at 380 mA (~100 V) for 30 minutes. After crosslinking at 120 mJ/cm², the
419 membrane was incubated in 15 ml of Blocking Buffer for 15 minutes with
420 gentle shaking. Then, the membrane was shifted to 15 ml of Blocking Buffer
421 with 7.5 μ l of Streptavidin-HRP Conjugate for 15 minutes with gentle shaking.
422 Transfer membrane to a new container and rinse it briefly with 20 ml of 1 X
423 wash solution. Wash membrane four times for 5 minutes each in 20 ml of 1 X
424 wash solution with gentle shaking. Transfer membrane to 20 ml of Substrate
425 Equilibration Buffer. Incubate membrane for 5 minutes with gentle shaking.

426 Transfer membrane to 5 ml of Substrate Working Solution for 5 minutes.
427 Expose membrane to a low-light cooled CCD imaging apparatus
428 (Tanon-5200).

429

430 **Gene expression analysis**

431 Total RNA was extracted using the RNAlant (Real-Times, China). cDNA was
432 synthesized by the use of PrimeScript™ RT reagent Kit with gDNA Eraser
433 (Perfect Real Time) according to the reverse transcription protocol (Takara).
434 The resulting cDNA was subjected to relative quantitative PCR using a SYBR
435 Premix Ex Taq™ kit (TaKaRa) on a Roche LightCycler 480 real-time PCR
436 machine, according to the manufacturer's instructions. The relative
437 expression of genes was normalized to that of *ACT2* and *PP2A*.

438

439 **Plasmid construction and generation of transgenic plants**

440 For construction of transient expression vectors, the GAL4 binding domain
441 was fused with mCherry containing a nuclear localization signal to generate
442 35S:BD-nmCherry. VP16, bHLH38, bHLH39, bHLH100 bHLH101 and FIT
443 were respectively fused with BD-nmCherry as the effectors. The pGAL4
444 promoter driving a GFP containing a nuclear localization signal was as the
445 reporter. For the subcellular localization assays, bHLH38, bHLH39, bHLH100
446 and bHLH101 were fused with mCherry respectively, and FIT was fused with
447 GFP. For the construction of *bhlh4x-1/FIToe* plants, the HA-tagged FIT driven
448 by 35S promoter was introduced into *bhlh4x-1* mutant by transformation.

449

450 **Chromatin immunoprecipitation (ChIP) assays**

451 ChIP assays were conducted according to previously described protocols
452 (Saleh et al., 2008). Plants grown on +Fe media for 7 days were shifted to
453 -Fe media for 3 days, and then whole seedlings were used for ChIP assays.
454 To quantify FIT-DNA binding ratio, qPCR was performed with the *TUB2* as the
455 endogenous control.

456

457 **Subcellular localization**

458 The full-length FIT was fused with GFP to generate FIT-GFP and the
459 full-length bHLH38/39/100/101 with mCherry to generate
460 bHLH38/39/100/101-mCherry. The plasmids above were transformed into
461 agrobacteria. Agrobacteria were incubated in LB liquid media. When growth
462 reached an OD600 of approximately 3.0, the bacteria were spun down gently
463 (3200 g, 5 min), and the pellets were resuspended in infiltration buffer (10 mM
464 MgCl₂, 10 mM MES, pH 5.6) at a final OD600 of 1.0. A final concentration of
465 0.2 mM acetosyringone was added. The agrobacteria were kept at room
466 temperature for at least 2 h without shaking. Leaf infiltration was conducted in
467 3-week-old *N. benthamiana*. Excitation laser wave lengths of 488 nm and 563
468 nm were used for imaging GFP and mCherry signals, respectively.

469

470 **Acknowledgments**

471 We thank the Biogeochemical Laboratory and Central Laboratory
472 (Xishuangbanna Tropical Botanical Garden) for assistance in the
473 determination of Fe concentration. We thank Germplasm Bank of Wild
474 Species in Southwest China for confocal laser scanning microscopy.

475

476 **Funding**

477 This work was supported by the Applied Basic Research Project of Yunnan
478 Province (2019FB028 and 202001AT070131) and the Youth Talent Support
479 Program of Yunnan Province (YNWR-QNBJ-2018-134).

480

481 **Conflict of interest statement**

482 None declared.

483 **References**

- 484 **Cai Y, Li Y, Liang G.** 2021. FIT and bHLH Ib transcription factors modulate
485 iron and copper crosstalk in Arabidopsis. *Plant Cell and Environment*
486 44:1679-1691.
- 487 **Colangelo EP, Guerinot ML.** 2004. The essential basic helix-loop-helix
488 protein FIT1 is required for the iron deficiency response. *The Plant Cell* **16**:
489 3400-3412.
- 490 **Fox TC, Guerinot ML.** Molecular biology of cation transport in plants. *Annu*
491 *Rev Plant Physiol Plant Mol Biol.* 1998 49:669-696.
- 492 **Grillet L, Schmidt W.** 2019. Iron acquisition strategies in land plants: not so
493 different after all. *New Phytologist* **224**: 11-18.
- 494 **Heim MA, Jakoby M, Werber M, Martin C, Weisshaar B, Bailey PC.** 2003.
495 The basic helix-loop-helix transcription factor family in plants: a
496 genome-wide study of protein structure and functional diversity. *Mol Biol*
497 *Evol.* 20: 735-747.
- 498 **Jakoby M, Wang HY, Reidt W, Weisshaar B, Bauer P.** 2004. FRU
499 (BHLH029) is required for induction of iron mobilization genes in
500 Arabidopsis thaliana. *FEBS Letters* **577**: 528-534.
- 501 **Lei R, Li Y, Cai Y, Li C, Pu M, Lu C, Yang Y, Liang G.** 2020. bHLH121
502 Functions as a Direct Link that Facilitates the Activation of FIT by bHLH IVc
503 Transcription Factors for Maintaining Fe Homeostasis in Arabidopsis. *Mol*
504 *Plant.* 13: 634-649.
- 505 **Liu Y, Li X, Li K, Liu H, Lin C.** 2013. Multiple bHLH proteins form
506 heterodimers to mediate CRY2-dependent regulation of flowering-time in
507 Arabidopsis. *PLoS Genetics.* **9**: e1003861.
- 508 **Maurer F, Naranjo Arcos MA, Bauer P.** 2014. Responses of a triple mutant
509 defective in three iron deficiency-induced Basic Helix-Loop-Helix genes of
510 the subgroup Ib(2) to iron deficiency and salicylic acid. *PLoS One* **9**:
511 e99234.
- 512 **Naranjo-Arcos MA, Maurer F, Meiser J, Pateyron S, Fink-Straube C,**

- 513 **Bauer P.** 2017. Dissection of iron signaling and iron accumulation by
514 overexpression of subgroup Ib bHLH039 protein. *Scientific Reports* **7**:
515 10911.
- 516 **Schwarz B, Bauer P.** 2020. FIT, a regulatory hub for iron deficiency and
517 stress signaling in roots, and FIT-dependent and -independent gene
518 signatures. *Journal of Experimental Botany* **71**: 1694–1705.
- 519 **Sivitz AB, Hermand V, Curie C, Vert G.** 2012. Arabidopsis bHLH100 and
520 bHLH101 control iron homeostasis via a FIT-independent pathway. *PLoS*
521 *One* **7**: e44843.
- 522 **Trofimov K, Ivanov R, Eutebach M, Acaroglu B, Mohr I, Bauer P,**
523 **Brumbarova T.** 2019. Mobility and localization of the iron
524 deficiency-induced transcription factor bHLH039 change in the presence of
525 FIT. *Plant Direct* **3**: e00190.
- 526 **Wang HY, Klatte M, Jakoby M, Bäumlein H, Weisshaar B, Bauer P.** 2007.
527 Iron deficiency-mediated stress regulation of four subgroup Ib BHLH genes
528 in Arabidopsis thaliana. *Planta* **226**: 897-908.
- 529 **Wang N, Cui Y, Liu Y, Fan H, Du J, Huang Z, Yuan Y, Wu H, Ling HQ.** 2013.
530 Requirement and functional redundancy of Ib subgroup bHLH proteins for
531 iron deficiency responses and uptake in Arabidopsis thaliana. *Molecular*
532 *Plant* **6**: 503-513.
- 533 **Wang S, Chen JG.** 2014. Regulation of cell fate determination by
534 single-repeat R3 MYB transcription factors in Arabidopsis. *Front Plant Sci.*
535 **5**:133.
- 536 **Yi Y, Guerinot ML.** 1996. Genetic evidence that induction of root Fe(III)
537 chelate reductase activity is necessary for iron uptake under iron deficiency.
538 *Plant Journal.* **10**: 835-844.
- 539 **Yuan YX, Zhang J, Wang DW, Ling HQ.** 2008. AtbHLH29 of Arabidopsis
540 thaliana is a functional ortholog of tomato FER involved in controlling iron
541 acquisition in strategy I plants. *Cell Research* **15**: 613-621.
- 542 **Zhang H, Li Y, Yao X, Liang G, Yu D.** 2017. POSITIVE REGULATOR OF

543 IRON HOMEOSTASIS1, OsPRI1, Facilitates Iron Homeostasis. *Plant*
544 *Physiology* **175**: 543-554.

545 **Zhang H, Li Y, Pu M, Xu P, Liang G, Yu D.** 2020. *Oryza sativa* POSITIVE
546 REGULATOR OF IRON DEFICIENCY RESPONSE 2 (OsPRI2) and
547 OsPRI3 are involved in the maintenance of Fe homeostasis. *Plant Cell and*
548 *Environment* **43**: 261-274.

549

550 **Supporting Information**

551 Additional Supporting Information may be found online in the Supporting
552 Information section at the end of the article.

553 **Supplemental Figure S1.** Comparison of *fit-2* and *bhlh4x* mutants.

554 **Supplemental Figure S2.** Transcripts responsive to Fe Deficiency in a FIT or
555 bHLH Ib dependent fashion in shoots.

556 **Supplemental Figure S3.** Phenotypes of *bhlh4x-2 fit-2* quintuple mutants.

557 **Supplemental Figure S4.** Expression of *IRT1* and *FRO2* in the roots of *FIT*
558 overexpression plants.

559 **Supplemental Table S1. Expression of Fe-deficiency responsive genes**
560 **in roots.**

561 **Supplemental Table S2. Expression of Fe-deficiency responsive genes**
562 **in shoots.**

563 **Supplemental Table S3.** Primers used in this paper.

564

Figure Legends

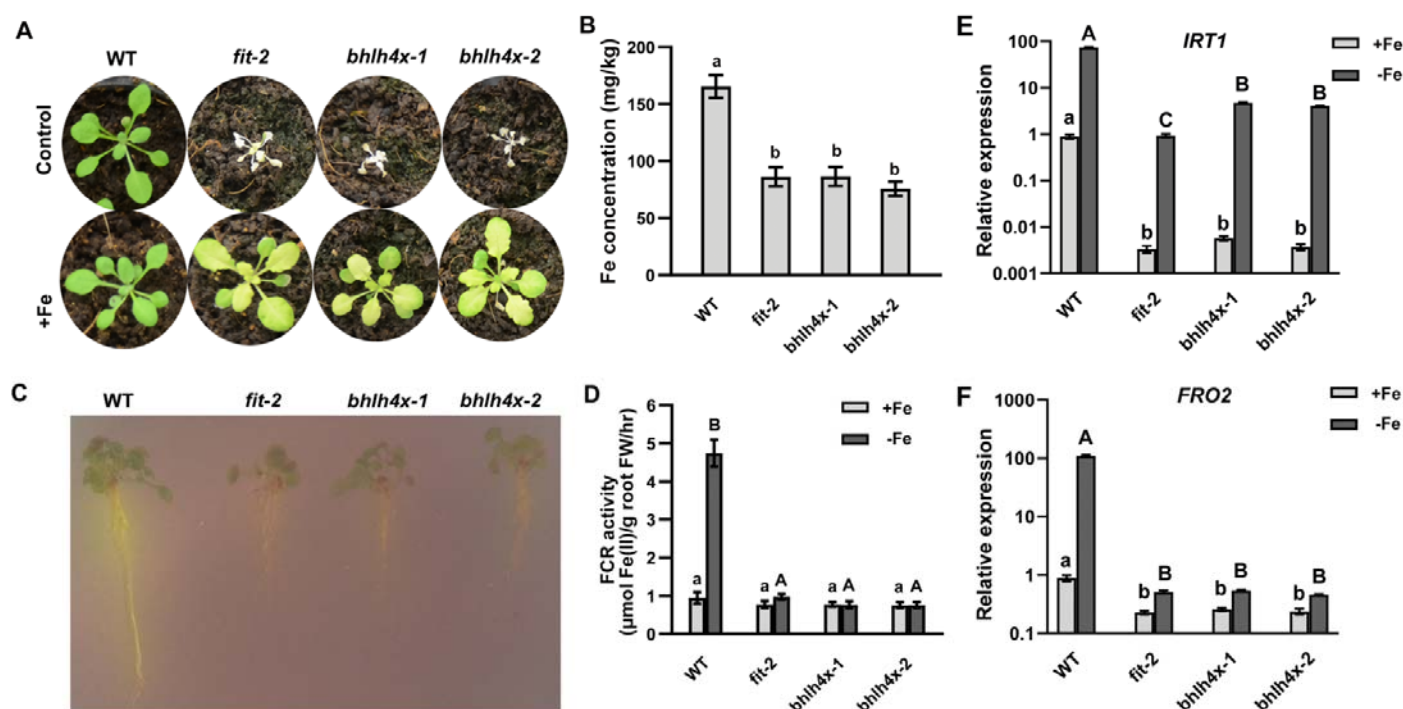


Figure 1. The Fe deficiency response of *fit-2* and *bhlh4x* mutants.

(A) Phenotypes of *fit-2* and *bhlh4x*. Four-week-old plants are shown. 'Control' indicates that plants were watered with tap water; '+Fe' indicates that plants were watered every three days with 0.5 mM Fe (II)-EDTA solution.

(B) Fe concentration. Plants were watered every three days with 0.5 mM Fe (II)-EDTA solution. Leaves from four-week-old plants were used for Fe measurement. Data represent means ± standard deviation (SD) ($n = 3$). Different letters above each bar indicate statistically significant differences as determined by one-way ANOVA followed by Tukey's multiple comparison test ($P < 0.05$).

(C) Rhizosphere acidification. Seedlings grown on +Fe medium for 5 days were shifted to -Fe medium for 3 days, and then shifted to plates containing bromocresol purple.

(D) FCR activity. Data represent means ± standard deviation (SD) ($n = 3$). Different letters above each bar indicate statistically significant differences as determined by one-way ANOVA followed by Tukey's multiple comparison test.

(E) and (F) Expression of *IRT1* (E) and *FRO2* (F) in *fit-2* and *bhlh4x*. Plants were grown on +Fe medium for 4 d and then transferred to +Fe or -Fe medium for 3 d. RNA was prepared from root tissues. Data represent means \pm standard deviation (SD) ($n = 3$). The different letters above each bar indicate statistically significant differences as determined by one-way ANOVA followed by Tukey's multiple comparison test ($P < 0.05$).

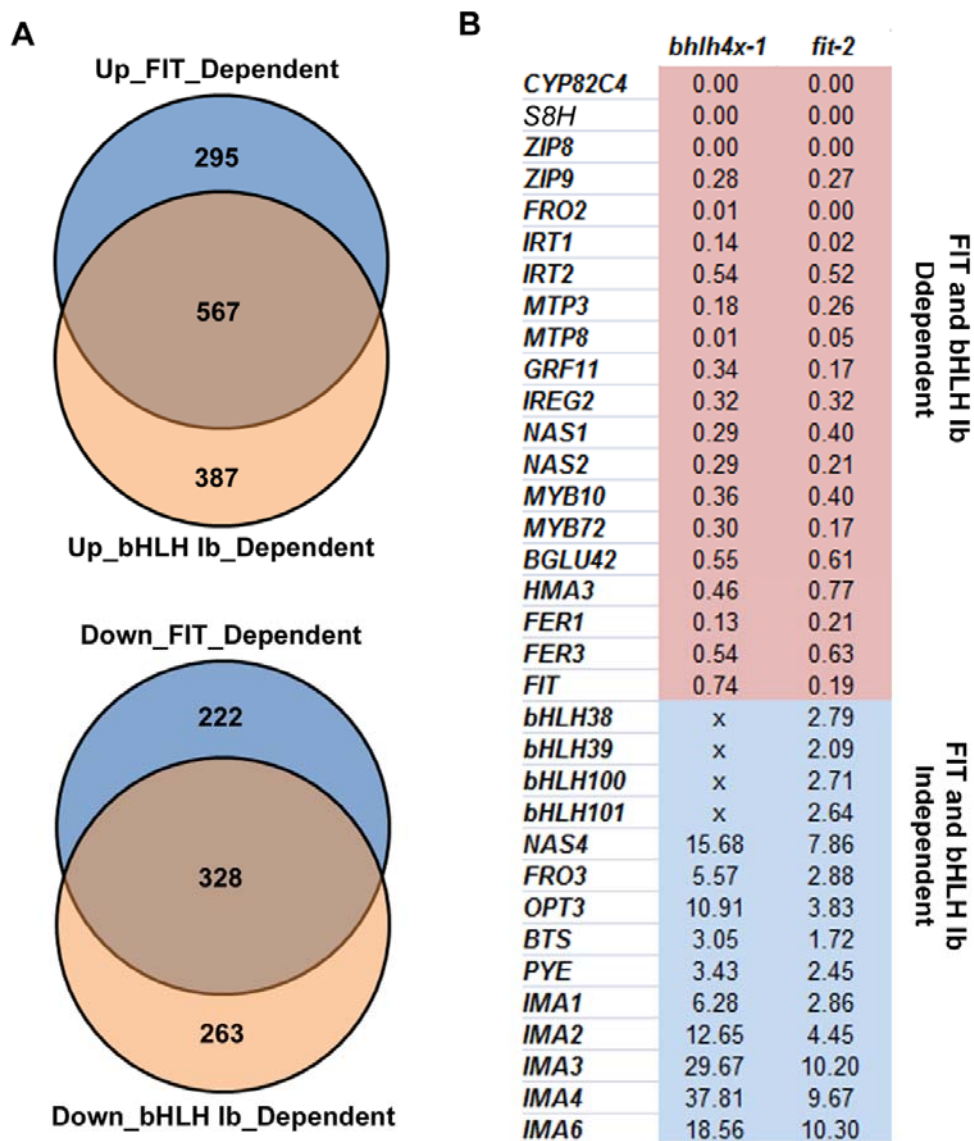


Figure 2. Expression of Fe deficiency responsive genes in the roots of *fit-2* and *bhlh4x-1*.

(A) Venn diagram showing overlap between FIT-dependent and bHLH Ib dependent genes.

(B) Relative transcript levels of genes involved in Fe deficiency response signaling in *fit-2* and *bhlh4x-1* under Fe-deficient conditions. The gene expression level in the wild type under Fe-deficient conditions was set to 1. Data are from the transcriptome in roots. “x” indicates that the RNA abundance for this gene is unavailable since the full-length CDS of *bHLH38/100/101* is undetectable and that of *bHLH39* is mutated.

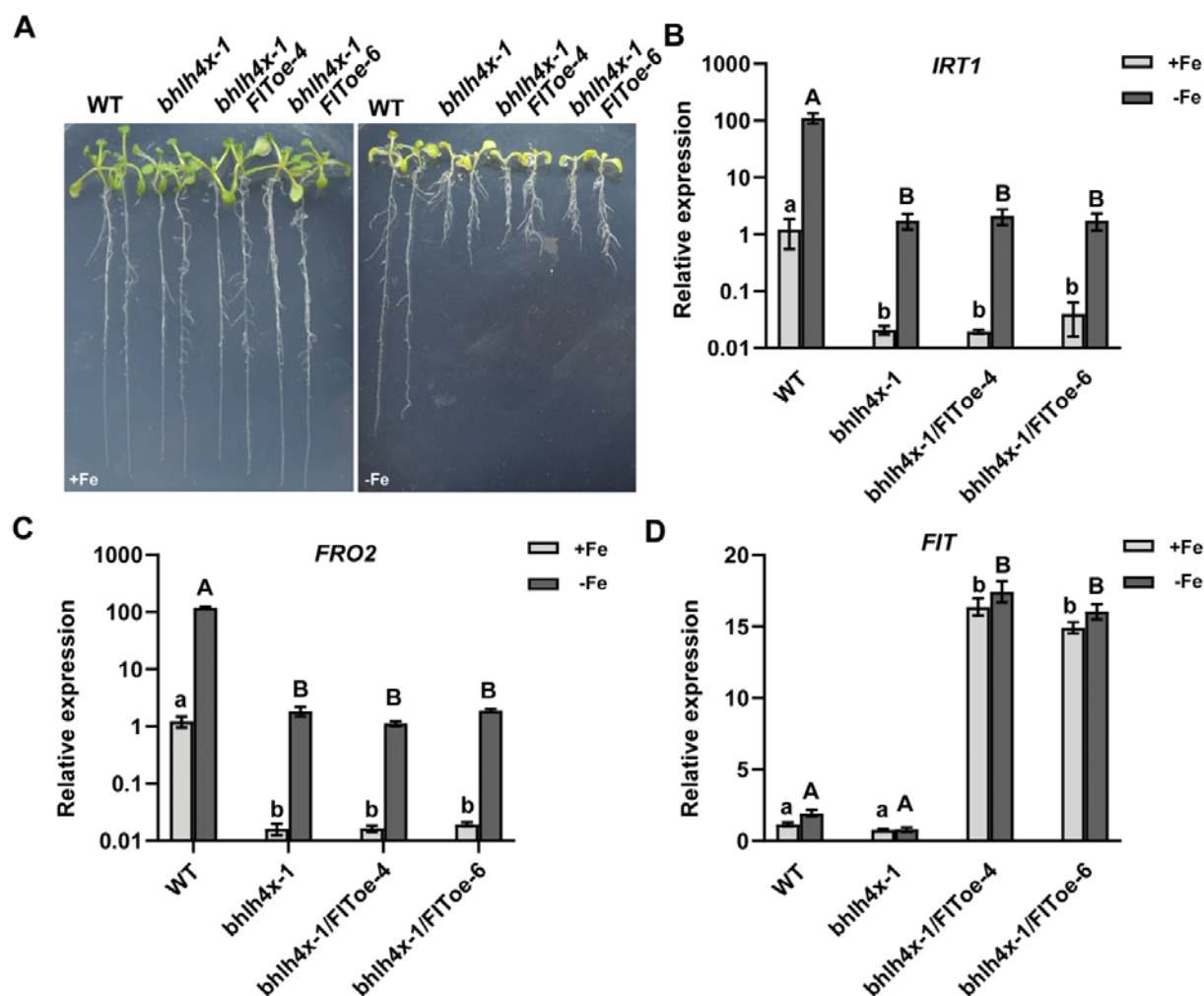


Figure 3. *FIT* overexpression does not rescue *bhlh4x-1*.

(A) Phenotypes of 10-day-old seedlings grown on +Fe or –Fe medium are shown.

(B-D) Expression of *IRT1* (B), *FRO2* (C) and *FIT* (D).

Plants were grown on +Fe medium for 4 d and then transferred to +Fe or –Fe medium for 3 d. RNA was prepared from root tissues. Data represent means \pm standard deviation (SD) ($n = 3$). The different letters above each bar indicate statistically significant differences as determined by one-way ANOVA followed by Tukey's multiple comparison test ($P < 0.05$).

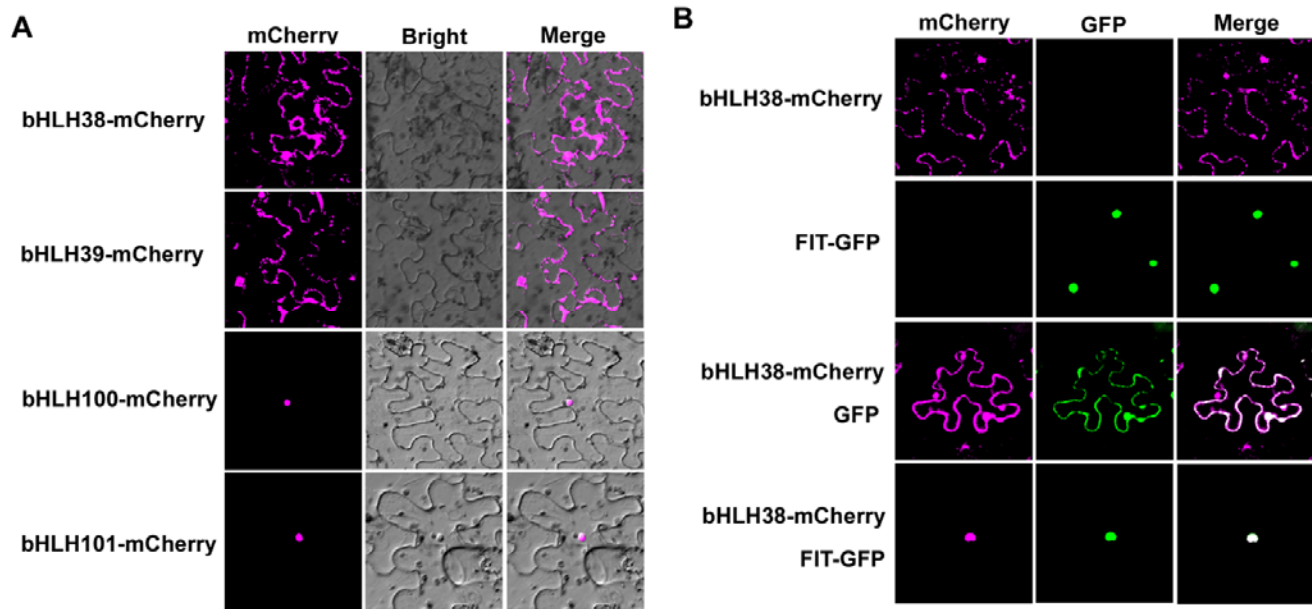


Figure 4. Subcellular localization of four bHLH Ib members.

(A) Subcellular localization of bHLH Ib. bHLH38-mCherry, bHLH39-mCherry, bHLH100-mCherry, or bHLH101-mCherry, were expressed transiently in tobacco cells.

(B) Effect of FIT on localization of bHLH38. bHLH38-mCherry, FIT-GFP, the combination of bHLH38-mCherry/GFP, and the combination of bHLH38-mCherry/FIT-GFP were expressed respectively in tobacco cells.

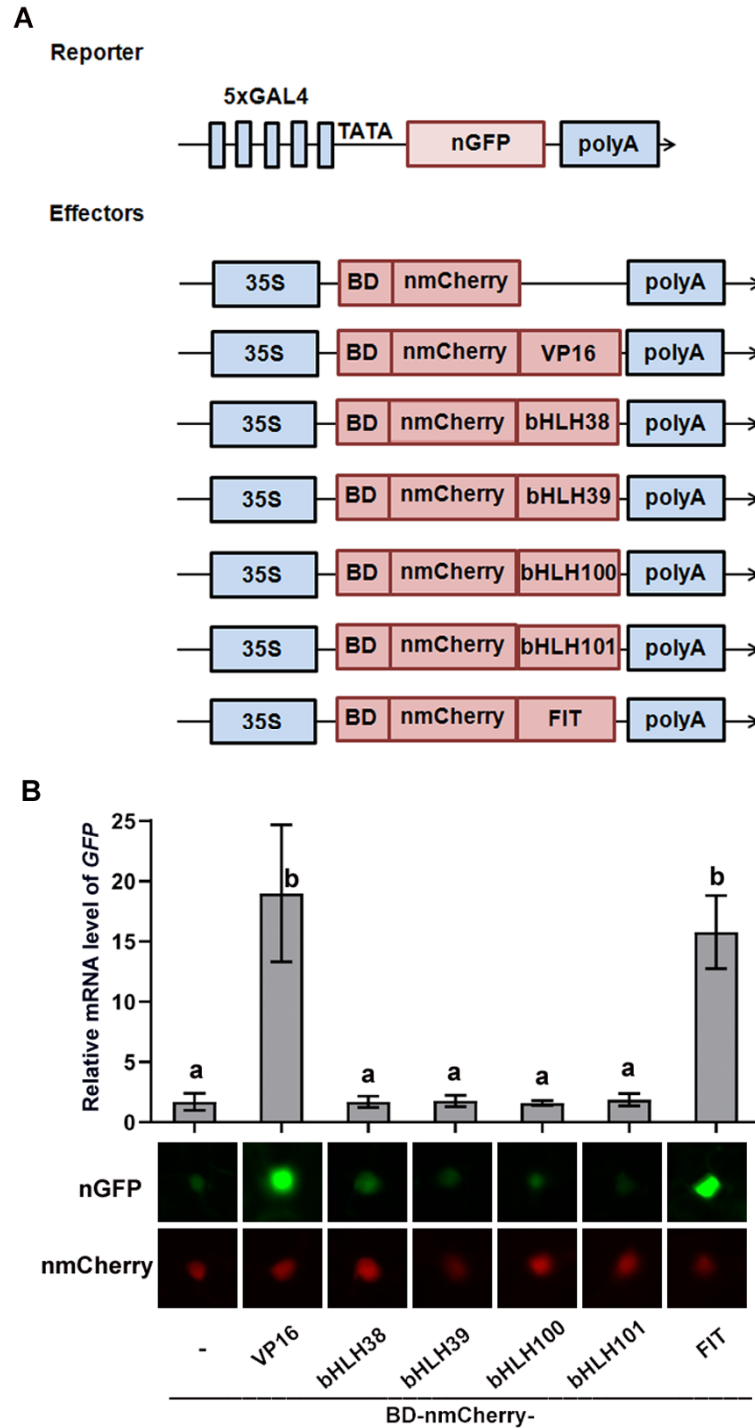


Figure 5. FIT has transcription activation ability.

(A) Schematic diagram of constructs used in transient expression assays in
(B) The reporter construct consists of five GAL4 binding motifs, a nuclear localization sequence tagged GFP (nGFP), and a poly(A) terminator. An

effector consists of cauliflower mosaic virus 35S promoter (35S), GAL4 DNA binding domain (BD), a nuclear localization sequence tagged mCherry (nmCherry), a test gene, and a polyA terminator. VP16, an established transactivation domain, was used as a positive control.

(B) Determination of transactivation activity. Representative GFP and mCherry signals for each combination are shown. Expression of *nGFP* was normalized to *NPT II*. Data represent means \pm standard deviation (SD) ($n = 3$). Different letters above each bar indicate statistically significant differences as determined by one-way ANOVA followed by Tukey's multiple comparison test.

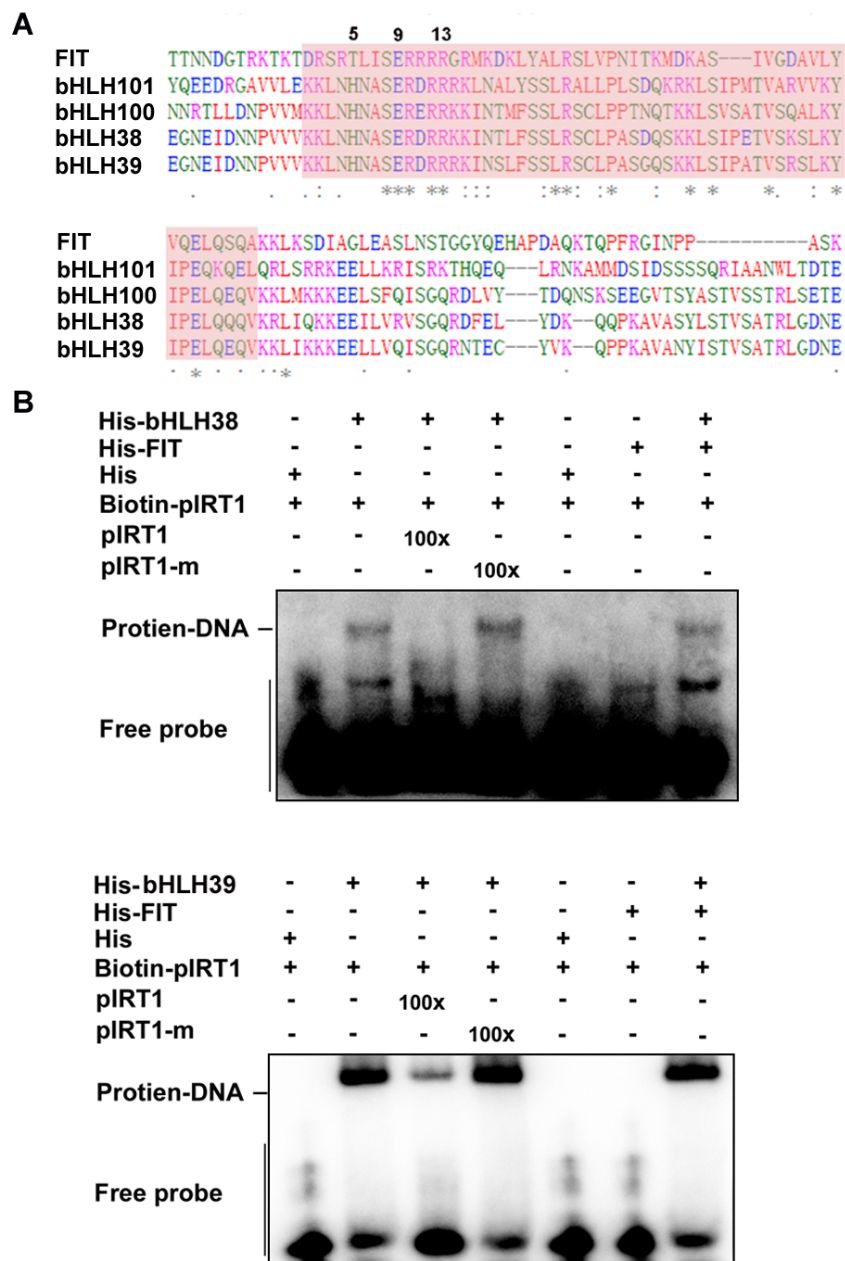


Figure 6. bHLH Ib TFs have DNA binding ability.

(A) Alignment of bHLH domains of FIT and bHLH Ib. The regions in shadow represent the bHLH domains. The numbers (5, 9 and 13) indicate the 5th, 9th and 14th residues of bHLH domain.

(B) EMSA assays. EMSAs were performed with a fragment of *IRT1* promoter. His-bHLH38, His-bHLH39, and His-FIT were used for binding assays. Biotin-probe, biotin-labeled probe; cold-probe, unlabeled probe; cold-probe-m, unlabeled mutated probe with mutated E-box.

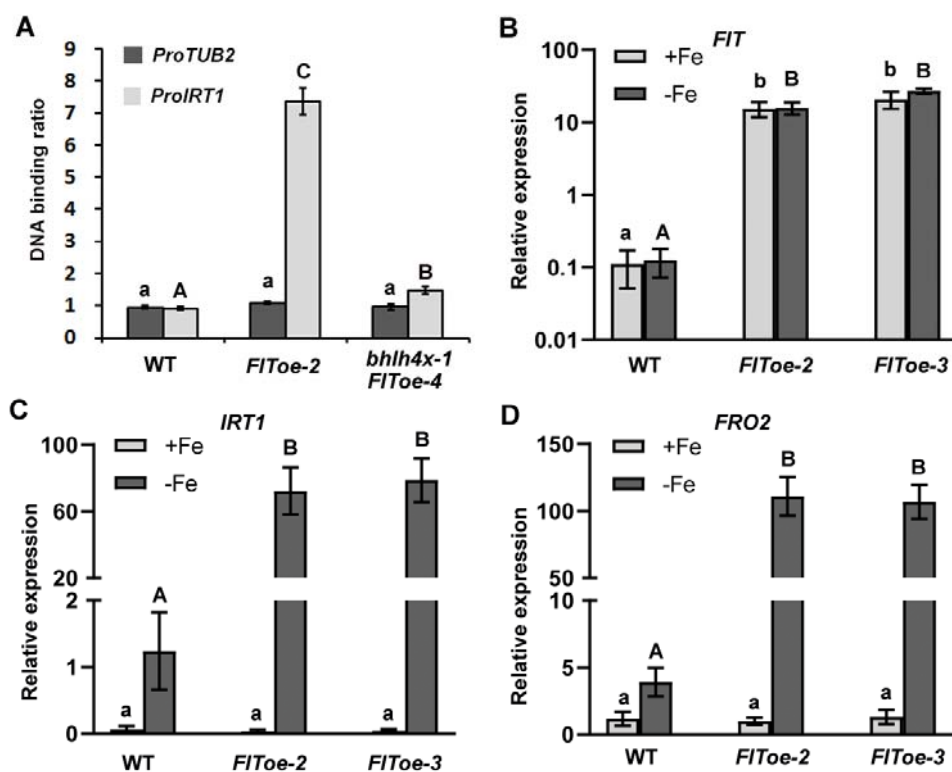


Figure 7. Association of FIT with the *IRT1* promoter requires bHLH 1b.

(A) ChIP assays. Seven-day-old seedlings grown on +Fe media were shifted to -Fe media for three days. Whole seedlings were harvested for ChIP assays using anti-HA antibody, and the immunoprecipitated DNA was quantified by qPCR. The binding of the *TUB2* promoter fragment in the wild type was set to 1 and used to normalize the DNA binding ratio of the *IRT1* promoter. Data represent means \pm SD ($n = 3$). The value which is significantly different from the corresponding control wild type was indicated by * ($P < 0.05$), as determined by Student's t test.

(B) Expression of *IRT1* and *FRO2* in the leaves of *FIT* overexpression plants. Plants were grown on +Fe medium for 4 d and then transferred to +Fe or -Fe medium for 3 d. RNA was prepared separately shoots. Data represent means \pm standard deviation (SD) ($n = 3$). The different letters above each bar indicate statistically significant differences as determined by one-way ANOVA followed by Tukey's multiple comparison test ($P < 0.05$).

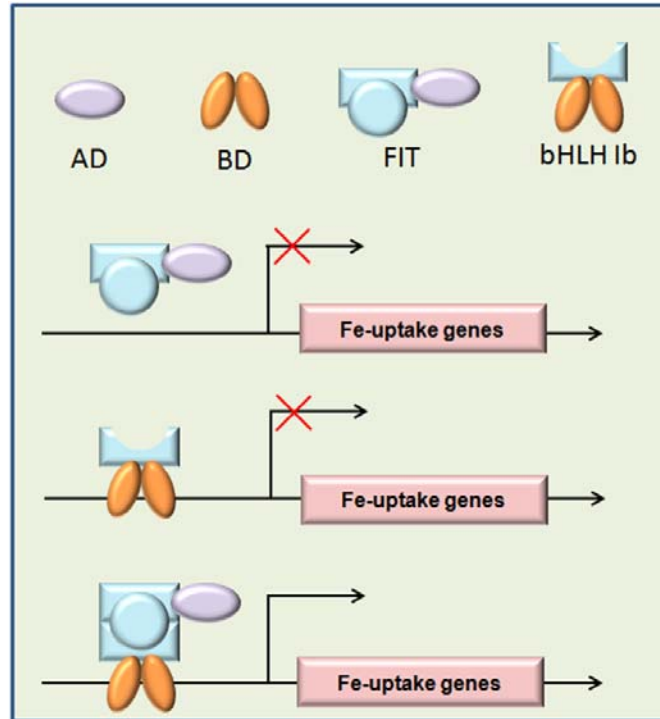


Figure 8. A proposed working model of FIT and bHLH Ib.

bHLH Ib has a DNA binding domain (BD) responsible for target recognition. FIT has a transcription activation domain (AD) responsible for transactivation. FIT and bHLH Ib form a functional transcriptional complex. FIT alone cannot bind to the promoters of Fe uptake genes, and bHLH Ib alone cannot initiate the transcription of Fe-uptake genes. The combination of FIT and bHLH Ib results in a functional complex to activate the transcription of Fe-uptake genes.